Journal of Sound and Vibration (1998) **217**(1), 163–182
Article No. sv981766

ON IMPROVING THE PERFORMANCE OF AUTOMOTIVE SEMI-ACTIVE SUSPENSION SYSTEMS THROUGH ROAD PREVIEW

T. J. GORDON AND R. S. SHARP

*Department of Aeronautical and Automotive Engineering and Transport Studies, Loughborough University, Loughborough LE*11 3*TU and School of Mechanical Engineering, Cranfield University, Bedford MK*43 0*AL, England*

(*Received* 22 *December* 1997, *and in final form* 27 *May* 1998)

A quarter car suspension system model containing a controllable damper with a limited range of coefficient values, a limited adjustment system bandwidth and a realistic elastic mounting to the car body is optimized for operation on a random road through a novel numerical method. The optimized system is simulated traversing random road surfaces and performance measures are extracted from the simulation runs. Comparisons are made with corresponding measures from relevant alternative systems. The effectiveness of the numerical optimization is established and conclusions are drawn on the usage and value of preview for semi-active automotive suspensions.

1. INTRODUCTION

Of the large number of research papers which have been concerned with computer controlled suspension systems for vehicles, a small proportion have discussed road preview. Bender [1] and Tomizuka [2] were pioneers in the field, each treating the optimization of one mass systems with perfect actuation. In cases involving active suspensions, the following have been established, largely by application of linear optimal control theory: (a) the potential benefits in performance to be obtained from preview; (b) the typical energy consumption costs; and (c) the amount of preview necessary as a function of vehicle speed, wheelbase and control bandwidth [3]. The results indicate that "look-ahead" preview control is not, at present, a viable technology for anything other than a small minority of applications. A rather large preview distance is needed for much benefit to be gained under normal operating conditions and gaining benefit from the preview is probably at the expense of energy consumption.

It has been established that the road elevation can be measured about 1 m ahead of the front of a car in normal service [4] but it is likely that the practical difficulties associated with obtaining the greater "look-ahead" distances needed will be considerable and the freely available "wheelbase" preview is useful only with a full bandwidth suspension. With preview, the actuators operate more vigorously on

0022–460X/98/410163 + 20 $30.00/0

a random road than without it [5], which implies greater energy consumption of an electro-hydraulic system of normal design. Note, however, that the opposite result can be obtained, depending on whether the calculations relate to idealised totally efficient and energy regenerative devices or to practical electro-hydraulic systems [6, 7].

"Wheelbase preview" is normally such that a slow-active or limited bandwidth suspension cannot gain significantly from the preview information. A full bandwidth system may so gain [5] but the full bandwidth design seems not practical in any case, due to its capital cost, weight, maintenance needs and energy requirements [8–10].

Preview control of a semi-active suspension can be useful in each of two ways. Firstly, the preview can be used to counter the possibly adverse influences on performance of actuation delays in the dampers. Secondly, it can be used, in principle, to improve the control strategy over that which is best for a non-preview system. However, the inverse relationship between performance improvement and energy consumption through preview [3, 5] suggests that the addition of preview information to a semi-active suspension may not yield much advantage. Also, it is quite widely believed that the optimal control strategy for a semi-active system is to mimic a linear optimal active system as closely as possible, employing so-called "clipped" optimal control [11, 12]. This would imply that strategic advantage from preview semi-active control is unlikely to be obtainable. Nevertheless, it is possible that the best control schemes for realistic semi-active systems (with operating delays) with preview, are sufficiently different from those yielded by application of the linear optimal theory that this suggestion is incorrect [13].

Using clipped optimal preview control, Hac and Youn [11] made performance calculations for a full bandwidth quarter car system for sinusoidal roads, discrete road bumps and randomly profiled roads and it was concluded that sufficient preview significantly benefits almost all aspects of suspension performance simultaneously. Dynamic programming techniques have been used by Muijderman *et al*. [14] to determine the state control of a two state, instantly switchable damper of a quarter car for discrete road bumps but no conclusions on the value of preview were reached. Muijderman *et al*. [15] later described an optimization method of "branch and bound" nature to derive a switching control for a two state damper with first order lag switching dynamics, under road preview. The controller's ability to contribute to a defined performance objective was demonstrated but improvement of a conventional fixed system appeared modest. Implementation of the scheme on a vehicle appears to be processor intensive, a new optimization being needed at each discrete time step.

It remains somewhat uncertain, therefore, what constitutes the optimal use of road preview information for a realistic semi-active automotive suspension system and what sort of benefits can be obtained from it. Shedding more light on these issues and, in particular, trying to quantify them, are the main thrusts of the present paper. At the beginning, a semi-active quarter car model containing some realistic design features is set up and a novel numerical procedure for optimizing its performance is described. The system is then simulated traversing randomly

profiled roads and comparisons are made with relevant alternative systems. Conclusions relate to the optimization technique used, to the use of available preview information in a semi-active scheme and to the performance advantages which can be gained from the use of the information.

2. SYSTEM MODEL AND OPTIMIZATION OF THE DAMPING CONTROL

2.1. MODELS

The quarter car model is shown diagrammatically in Figure 1. The representations of body mass, wheel mass and tyre spring are conventional, while the damper is mounted in series with a relatively stiff spring, has second order actuation dynamics and is controllable via the damper coefficient demand signal, u, within the range 0 to 100 as illustrated in Figure 2, which shows the non-linear map: $F_{\text{damp}} = \mu(v, \bar{u}) = (200 + 48\bar{u}) \arctan(2v)$, where v is the relative velocity between the ends of the damper and $\bar{u}$ is the output of the second order signal filter shown in Figure 1. With the constraint on u, it is possible for $\bar{u}$ to take values outside the range 0 to 100 but with the high damping factor of the filter, the tendency to overshoot the demand u is rather small.

Other versions of the quarter car, which are of interest from a comparison point of view, are an infinite bandwidth linear active system, and a simple linear passive system with non-compliant damper mounting. The controllable suspensions will be subject to differing amounts of road surface preview. For the active system without preview, Linear Quadratic Regulator (LQR) or Linear Quadratic Gaussian (LQG) techniques [16] can be used to find a control which minimizes a quadratic cost function under white noise derived excitation and it is such a system which has been presumed here. For the active system with infinite preview,

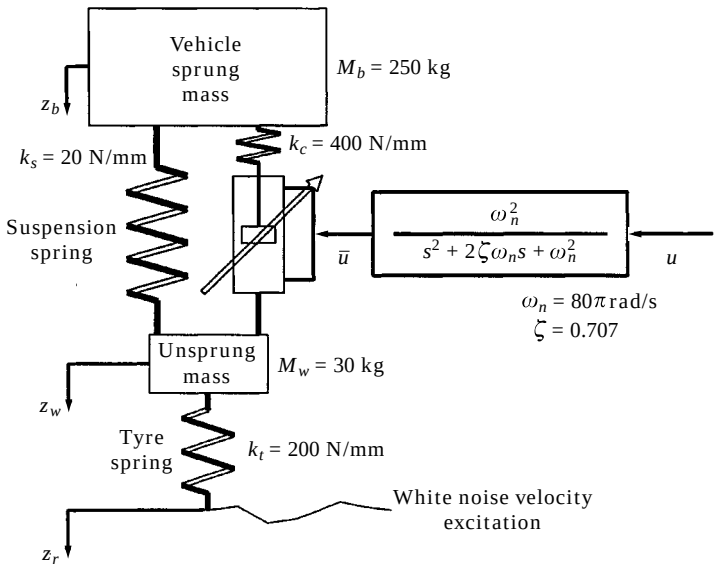

Figure 1. Diagrammatic representation of quarter-car suspension.

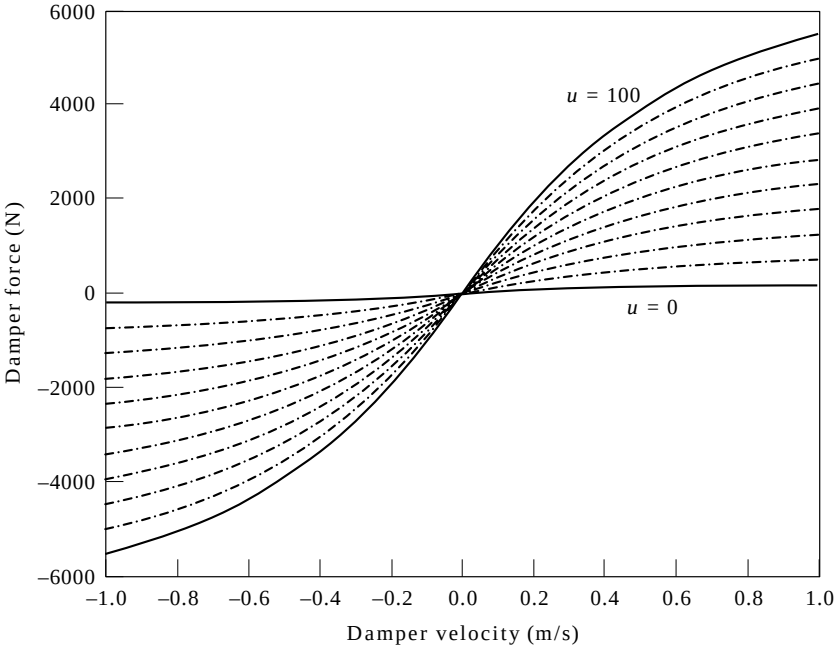

Figure 2. Steady state damper force/velocity map.

a new derivation of its frequency response functions in analytical form follows. From these response functions, it is straightforward to calculate responses to any defined excitation.

2.2. RESPONSES OF AN INFINITE BANDWIDTH ACTIVE SUSPENSION WITH INFINITE ROAD PREVIEW

With reference to the quarter-car model of Figure 1, if dynamic suspension force $F_s(t)$ is applied directly by an idealized actuator, replacing the spring and damper, the equations of motion are simply

$$M_b\ddot{z}_b = F_s(t), \qquad M_w\ddot{z}_w = k_t(z_r - z_w) - F_s(t). \tag{1}$$

The control objective is to choose $F_s(t)$ to minimize a standard form of quadratic cost function

$$C(T) = \frac{1}{T}\int_0^T \{\ddot{z}_b^2 + \alpha(z_r - z_w)^2 + \beta(z_w - z_b)^2\}\,\mathrm{d}t \tag{2}$$

in the limit as $T \to \infty$, where $\alpha > 0$, $\beta > 0$ are weighting parameters whose values are taken from an earlier paper [17], namely $\alpha = 116\,000$ and $\beta = 1190$. In the infinite preview case, it is assumed that $z_r(t)$ is explicitly known before the optimization is carried out.

It is well known that such a linear quadratic dynamic optimization can be formulated as a linear two point boundary value problem [18]. This means that a general solution can be expressed in terms of component sinusoids, found from

a Fourier analysis of $z_r(t)$. Thus, restricting attention to a sinusoidal road profile of wavelength λ, one can assume

$$z_r(t) = R\,\mathrm{e}^{\mathrm{j}\omega t}, \tag{3}$$

where $R(\omega)$ is a complex amplitude, $\omega = vel/\lambda$, and vel is the forward speed of the vehicle.

In steady state, the optimal control input and system responses are also sinusoidal,

$$F_s(t) = U\,\mathrm{e}^{\mathrm{j}\omega t}, \qquad z_w(t) = W\,\mathrm{e}^{\mathrm{j}\omega t}, \qquad z_b(t) = B\,\mathrm{e}^{\mathrm{j}\omega t}, \tag{4}$$

and again $U(\omega)$, $W(\omega)$ and $B(\omega)$ are complex scalars. Substituting these response forms in equations (1) yield,

$$-\omega^2 M_b B = U, \qquad -\omega^2 M_w W = k_t(R - W) - U. \tag{5}$$

It is clear that the minimization of $C(T)$ can be carried out over a single cycle, of duration $T_0 = 2\pi/\omega$. This results in a simplified cost function,

$$C(T_0) = \tfrac{1}{2}\{|B|^2\omega^4 + \alpha|R - W|^2 + \beta|W - B|^2\}, \tag{6}$$

where the real parts of the complex sinusoids have been taken and use has been made of the general formula

$$\frac{1}{T_0}\int_0^{T_0} [\mathrm{Re}\,(A\,\mathrm{e}^{\mathrm{j}\omega t})]^2\,\mathrm{d}t = \tfrac{1}{2}|A|^2. \tag{7}$$

The optimal control problem now reduces to the minimization of equation (6), subject to the constraints imposed in equations (5). Though Lagrange multipliers may be used, it is simpler to eliminate the constraints W and B from equation (6) by using equations (5) to give

$$2C(T_0) = M_b^{-2}|U|^2 + \frac{\alpha}{(k_t - M_w\omega^2)^2}\,|U - M_w\omega^2 R|^2 + \frac{\beta}{M_b^2\omega^4(k_t - M_w\omega^2)^2}\,|k_t M_b\omega^2 R + (k_t - M_T\omega^2)U|^2, \tag{8}$$

where $M_T = M_b + M_w$ is the total mass of the quarter-car. To minimize the expression with respect to the complex control amplitude U, it is possible to re-write it explicitly in terms of U and its complex conjugate $\tilde{U}$, treat these as independent variables and apply the condition [19]

$$\partial C/\partial\tilde{U} = 0, \tag{9}$$

which gives

$$M_b^{-2}U + \frac{\alpha(U - M_w\omega^2 R)}{(k_t - M_w\omega^2)^2} + \frac{\beta(k_t - M_T\omega^2)[k_t M_b\omega^2 R + (k_t - M_T\omega^2)U]}{M_b^2\omega^4(k_t - M_w\omega^2)^2} = 0.$$

After some algebraic manipulation:

$$\frac{U}{R} = \frac{M_b\omega^2\{\alpha M_b M_w\omega^4 - \beta k_t(k_t - M_T\omega^2)\}}{(k_t - M_w\omega^2)^2\omega^4 + \alpha M_b^2\omega^4 + \beta(k_t - M_T\omega^2)^2}, \tag{10}$$

from which one can assign the notation

$$H_1(\omega) = N_1(\omega)/D(\omega). \tag{10a}$$

For a general road input, $H_1(\omega)$ represents the frequency response for the optimal previewed control force, relative to the road vertical deflection input $z_r(t)$. From equations (5), the following related responses are easily obtained:

$$H_2(\omega) = \frac{R - W}{R} = \frac{-\omega^2\{(k_t - M_w\omega^2)M_w\omega^4 + \beta(k_t - M_T\omega^2)M_T\}}{D(\omega)}, \tag{11}$$

$$H_3(\omega) = \frac{W - B}{R} = \frac{\omega^4\{k_t(k_t - M_w\omega^2) + \alpha M_b M_w\}}{D(\omega)}. \tag{12}$$

H_2 and H_3 are respectively the frequency responses for suspension deflection and tyre deflection under the optimal preview controller. Though not directly suitable for controller synthesis—there is no explicit resolution into feedback and feedforward control components—these expressions are very useful for comparison with the numerical results derived below.

The above analytic formulae are applicable to any input profile $z_r(t)$. However, if as a reference we assume that the vertical contact velocity $\dot{z}_r(t)$ is a unit amplitude white noise process, the expected cost (ensemble average of $C(T)$ as $T \to \infty$) is given by

$$\hat{C} = \frac{1}{2\pi}\int_0^\infty P_c(\omega)\,\mathrm{d}\omega \tag{13}$$

where

$$P_c(\omega) = M_b^{-2}P_1(\omega) + \alpha P_2(\omega) + \beta P_3(\omega) \tag{14}$$

is the power spectral density associated with the cost function in equation (2) and

$$P_i(\omega) = \left|\frac{H_i(\omega)}{\omega}\right|^2, \qquad i = 1, 2, 3, \tag{15}$$

are the power spectra associated with the control force, tyre deflection and suspension deflection respectively. The system having these ideal responses is referred to as *ACI* in the results section.

Bender's results for infinite preview [1] can easily be recreated from equations (10), (11) and (12) but the inverse process, in which Bender's method is used to try to obtain the above expressions is fraught with algebraic complexity.

2.3. NUMERICAL OPTIMIZATION OF THE PREVIEW CONTROL SYSTEMS

To optimize the semi-active system, a numerical procedure has been devised, based on Pontryagin's Hamiltonian formulation of the non-linear optimal regulator; the method has been developed from those described in references [20] and [21] and it incorporates a novel use of passive suspension dynamics to provide approximate final-time boundary conditions. The scheme is to be applied to both the ideal active and detailed semi-active models, each with variable amounts of road preview. The method is now described in a general context, with case-specific details given in the Appendix.

The dynamic equations are written in state-variable form,

$$\dot{x} = f(x, u(t), w(t)), \tag{16}$$

where $u(t)$ is the control (control force in the active case, or command signal to the semi-active controllable damper) and $w(t) = \dot{z}_r(t)$ is the input disturbance. Control system optimization is considered to take place in real time, with a receding horizon for the preview control. At time t_0 and with preview time t_p, the available dynamic model becomes

$$\dot{x} = f(x, u(t), \hat{w}(t, t_0 + t_p)) \tag{17}$$

where

$$\hat{w}(t, \tau) = \begin{cases} w(t) & \text{if} \quad t \leqslant \tau \\ 0 & \qquad\quad t > \tau \end{cases} \tag{18}$$

is the previewed disturbance, assumed to be zero beyond the preview horizon.

Thus, upon assuming only finite preview is available, the optimization problem must be modified from the form of equation (2), with the performance index now being written

$$C(t_0, u(.)) = \int_{t_0}^{\infty} L(x, u(t), \hat{w}(t, t_0 + t_p))\, \mathrm{d}t, \tag{19}$$

where $L(x, u(t), \hat{w}(t, t_0 + t_p))$ is the underlying cost function—see the Appendix.

The notation $u(.)$ denotes the fact that C is a functional, depending on the entire control sequence $\{u(t)\colon t_0 < t < \infty\}$. A rigorous solution of the optimization problem is available through Pontryagin's Maximum Principle [18]. The Hamiltonian function is

$$H(x, p, u, \hat{w}) = p^{\mathrm{T}} f(x, u, \hat{w}) + L(x, u, \hat{w}) \tag{20}$$

in which the costate vector p satisfies the differential equations

$$\dot{p} = -\partial H / \partial x. \tag{21}$$

Ideally, the optimal control $u(t)$ is chosen to minimize the Hamiltonian at each instant of time, and the state and costate vectors satisfy the two-point boundary conditions

$$x(t_0) = x_0, \qquad \lim_{t \to \infty} p(t) = 0. \tag{22}$$

To make the optimization problem more tractable, one can reformulate it to depend on a reduced set of control parameters. Firstly, $u(t)$ is to operate as a discrete-time signal via a zero-order hold—a hold interval $\Delta = 5$ ms being used here. Secondly, $u(t)$ is optimized over a finite time interval $(t_0, t_0 + t_h)$, where t_h represents an optimization horizon; see Figure 3.

It turns out that t_h can be made reasonably small—$t_h = 1$ s in the suspension optimization—provided some account is taken of the system dynamics beyond the final time $t_0 + t_h$. This is achieved by using a simpler linear passive suspension model of the form

$$\dot{x} = Ax \tag{23}$$

to represent the final settling of the system with zero disturbance assumed. The cost function can be resolved as a quadratic function in the states,

$$L_{\text{passive}} = \tfrac{1}{2} x^{\mathrm{T}} Q x \tag{24}$$

in which case the total cost is approximated as

$$\begin{aligned} C(t_0, u(.)) &= C_1(t_0, u(.)) + C_2(x(t_0 + t_h)) \\ &= \int_{t_0}^{t_0 + t_h} L(x, u, \hat{w})\, \mathrm{d}t + \int_{t_0 + t_h}^{\infty} \frac{1}{2} x^{\mathrm{T}} Q x\, \mathrm{d}t. \end{aligned} \tag{25}$$

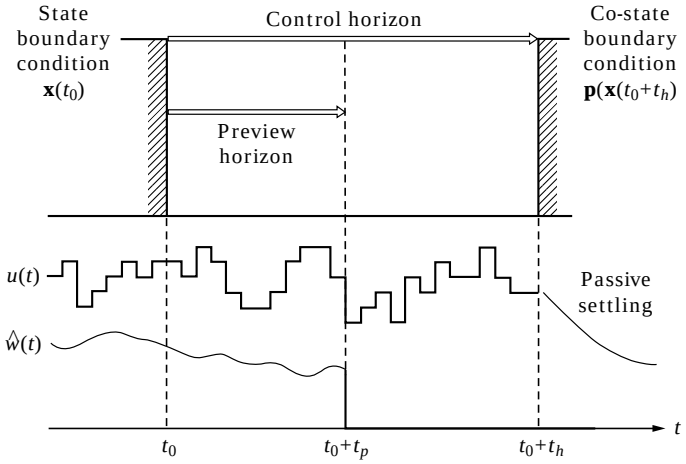

Figure 3. Timing structure of the numerical optimization.

The second integral is independent of any controls, or indeed the absolute time $t_0 + t_h$. It can be evaluated as

$$C_2(x) = \int_{t_0 + t_h}^{\infty} \frac{1}{2} x^{\mathrm{T}} Q x \, \mathrm{d}t = \tfrac{1}{2} x^{\mathrm{T}} P x, \tag{26}$$

where P is found from the Lyapunov matrix equation

$$A^{\mathrm{T}} P + P A + Q = 0. \tag{27}$$

Optimization then takes place over the time interval $(t_0, t_0 + t_h)$ by using a finite number of discrete-time controls and the revised boundary conditions:

$$x(t_0) = x_0; \qquad p(t_0 + t_h) = P x(t_0 + t_h). \tag{28}$$

One can now summarize the optimization process. From any given "initial" state $x(t_0) = x_0$, and a candidate set of controls

$$U = \{u_1, u_2, \ldots, u_N\}, \tag{29}$$

the state equations (17) are integrated forwards in time over the optimization interval, the co-state boundary conditions are then imposed, and then equations (21) are integrated in reverse time to evaluate the co-state vector. The gradient of the total cost $C(t_0, U)$ is given via the Hamiltonian as:

$$\frac{\partial C(t_0, U)}{\partial u_i} = \int_{t_i}^{t_{i+1}} \frac{\partial H}{\partial u_i} \, \mathrm{d}t, \tag{30}$$

where (t_i, t_{i+1}) is the hold interval associated with the ith control in U. From this, a simple steepest descent process is very effective at finding a numerical approximation to the set of optimal controls.

The efficiency of the integration process depends critically on the use of a discretized control signal, and the reduction of numerical integration time afforded by the use of passive co-states. Once an optimal set of controls has been found at time t_0, equations (16) are then available for forwards time integration over the hold interval $(t_0, t_0 + \Delta)$ with

$$u(t) = u_1 = \text{const}, \tag{31}$$

at which point the candidate controls may be simply amended, typically as

$$U' = \{u_2, \ldots, u_N, 0\}, \tag{32}$$

and the optimization process is repeated. It turns out that only a very small number of iterations is required for the optimization at each stage, since the new candidate control sequence U' is very close to optimal; this is especially true for the preview controller, since the system's dynamic evolution has already been anticipated in the earlier optimization.

Validation of the total optimization procedure will be carried out by reference to the fully active system. In particular, choosing $t_h = 1$ s implies a maximum preview horizon at $t_p = 1$ s also (see Figure 3). For the maximum preview case, the analytic results of section 2.2 can be used. Also, for $t_p = 0$ the standard LQR system is available for comparison.

2.4. TERMINOLOGY

Various system types have already been mentioned in the above and it is worth introducing some simple labels by which they can be known, as follows:

AC0, active LQR controlled system with zero preview;
ACI, unrestricted active system with infinite preview having ideal frequency response characteristics;
ACN0, active system without preview optimized numerically;
ACN1, active system with preview, having its control law numerically optimized: $t_p = 1$ s unless stated otherwise;
SAN0, semi-active system without preview with control law numerically optimized;
SAN1, similar to *SAN0* but with preview: $t_p = 1$ s unless stated otherwise.

Additionally, we shall investigate the question of whether a "clipped" optimal active control represents an acceptable approximation to the optimal semi-active control law. For the above numerical optimization process, this simply means that equation (17) is based on the simpler active system dynamics. The damper control, to be applied in the actual forward simulation of the semi-active system, is set to provide a closest available approximation to the required suspension force—upon taking into account the contribution of the spring force but ignoring the damper actuation transients. Thus we shall consider two further systems:

CSN0, clipped control of the semi-active system, optimized numerically for $t_p = 0$;
CSN1, clipped control of the semi-active system, optimized numerically for $t_p = 1$, unless stated otherwise.

3. SIMULATION RESULTS

Results are first generated to demonstrate the validity of the numerical optimization method in two cases for which the true optimal system is known, namely, the LQR controlled active system without preview, *AC0*, and the infinite preview unrestricted active system case treated analytically in the previous section, *ACI*. For the first of these cases, almost identical time histories, under a white noise vertical road velocity disturbance, are shown in Figure 4. For the second case, results are shown in Figure 5 in the form of output spectral densities, under the same excitation. The differences between the numerically obtained and the analytically obtained results are marginal. It appears appropriate to conclude that the numerical optimization is working well for these cases, with the implication that it is also effective for the semi-active cases, for which no direct checks are available. Output spectral densities for the systems *ACN1*, *SAN1* and *CSN* for

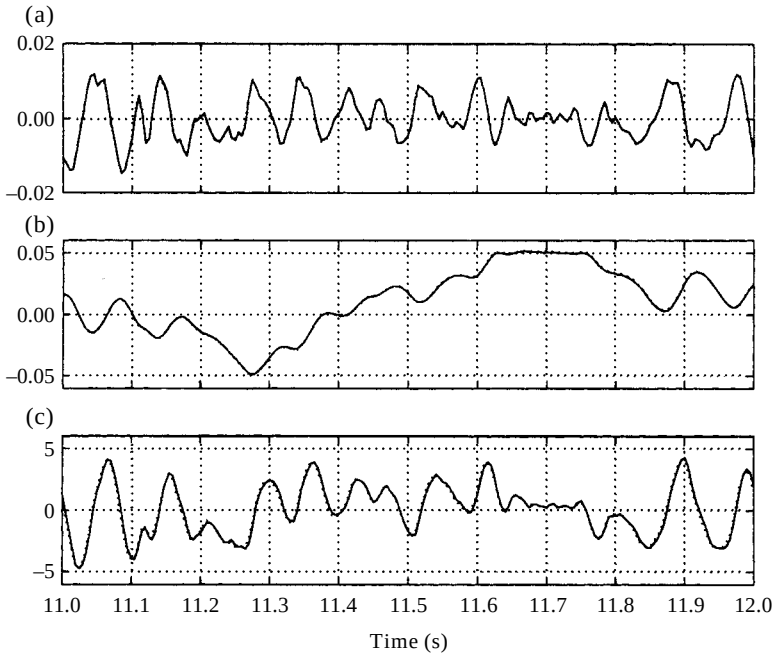

Figure 4. Motions of the quarter car under white noise road vertical velocity excitation for *AC0* (——) and *ACN0* (· · · · ·) systems. (a) Tyre deflection (m); (b) suspension deflection (m); (c) body acceleration (m s^{-2}).

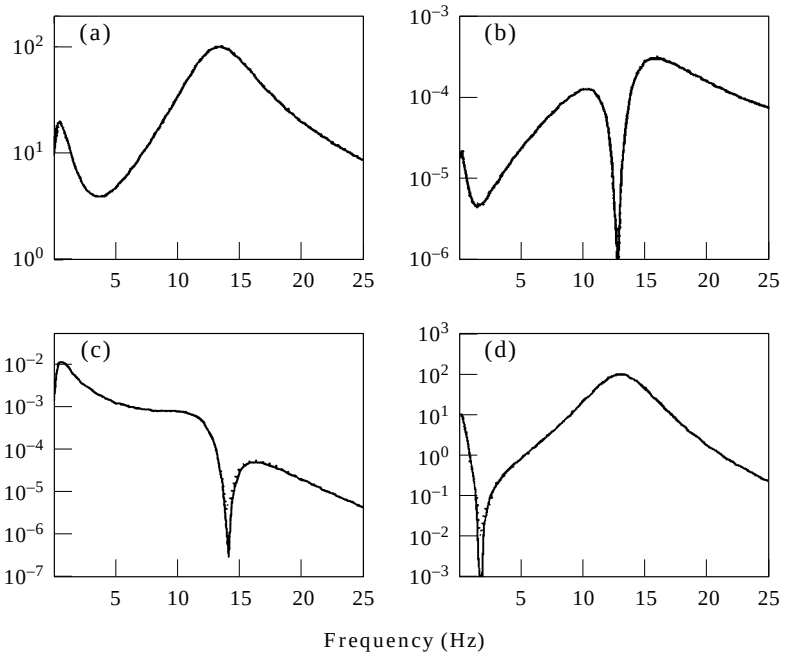

Figure 5. Output spectral densities of systems *ACI* (——) and *ACN1* (· · · ·) under white noise road vertical velocity excitation. (a) Total cost (1/Hz); (b) tyre deflection (m^2/Hz); (c) suspension deflection (m^2/Hz); (d) body acceleration ((m s^{-2})^2/Hz).

white noise road vertical velocity excitation are shown in Figures 6, 7 and 8 respectively. Preview times, in each case, are varied between 0 and 1 s.

Figures 9, 10 and 11 contain the corresponding root mean square (RMS) values of the response variables and also the cost function. "bva" denotes the body vertical acceleration $\ddot{z}_b$, "sws" the suspension working space $z_w - z_b$, "dtl" is $z_r - z_w$, which is (proportional to) dynamic tyre load and "total" denotes the RMS value associated with the overall cost function, i.e., $\sqrt{C(T)}$—see equation (2).

The general performance properties of active quarter car suspensions with different amounts of preview are known from previous research [3, 22] and the active system results in Figures 6 and 9 are entirely consistent with this prior knowledge. This further reinforces the idea that the numerical optimization is indeed deriving optimal configurations. Corresponding direct checks on the accuracy of the semi-active system optimizations cannot, of course, be made. However, it has been observed previously that, for zero preview, a "clipped optimal" semi-active quarter-car suspension for a random road disturbance input behaves much the same as a fully active suspension, hardly needing to "clip" at all [23]. In keeping with this, the present results show the overall cost of the optimal semi-active system without preview to be only a little higher than that of the active system. This is despite the fact that the notional active system has infinite bandwidth and unlimited force capabilities, while the semi-active system is bounded as shown in Figure 2.

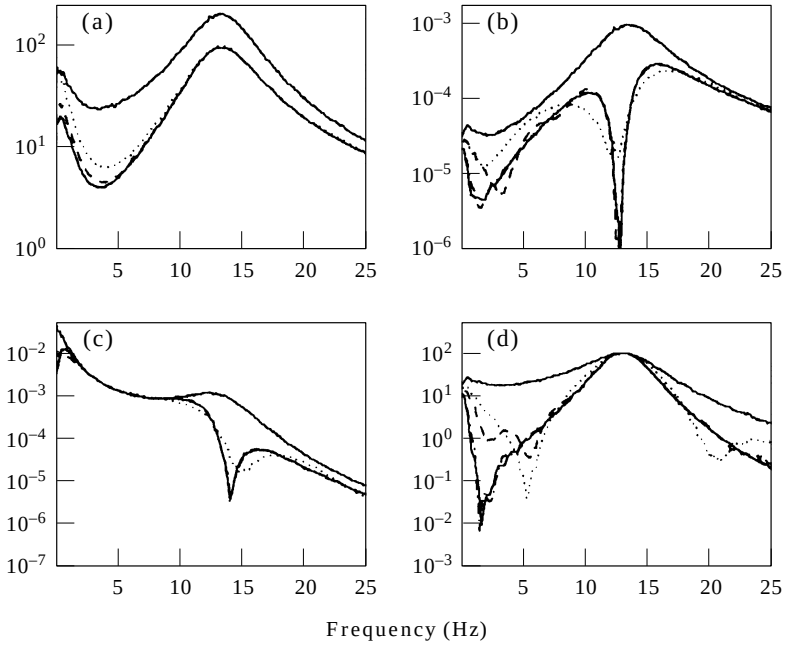

Figure 6. Output spectral densities for *ACN1* system under white noise road velocity excitation for preview times (s) 0 (——), 0·1 (· · · ·), 0·25 (——), 0·5 (·–·–), 1·0 (——). (a) Total cost (1/Hz); (b) tyre deflection (m^2/Hz); (c) suspension deflection (m^2/Hz); (d) body acceleration ($(m\ s^{-2})^2$/Hz).

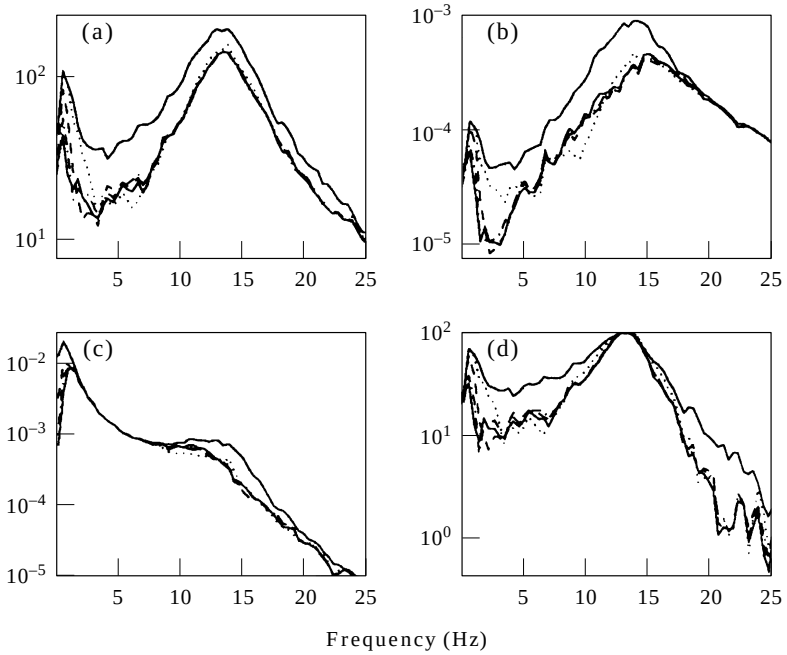

Figure 7. Output spectral densities for *SAN1* system under white noise road velocity excitation for preview times (s) 0 (——), 0·1 (· · · ·), 0·25 (——), 0·5 (·–·–), 1·0 (——). (a) Total cost (1/Hz); (b) tyre deflection (m^2/Hz); (c) suspension deflection (m^2/Hz); (d) body acceleration $((m\ s^{-2})^2$/Hz).

The bar charts of Figures 9–11, containing summary results, show that preview brings progressive advantage to all three types of system in respect of each aspect of performance. The value of preview to the active system is substantially greater than to the semi-active systems, and the "clipped" systems (CSN) lose ground progressively in comparison with the truly optimal (within the constraints described) semi-active systems (SAN) as the preview increases. In each case, most of the performance gain from preview comes from the first 0·1 s and the main part of the advantage is associated with better tyre load control. It is clear physically, and from prior results [3, 22], that these factors depend on the high damper control bandwidth of 40 Hz. If this were not so high, short previews would not be so useful and the wheel control would not be improved so much. Nevertheless, a preview time of 0·1 s is by no means trivial in practice, corresponding to 3 m preview distance at the reasonable vehicle speed of 30 m/s.

The results in Figures 6–8 reveal the frequencies at which particular advantage accrues from the optimal or near optimal use of the various previews. These results naturally confirm that little advantage is obtained, in these cases, when the preview time is extended beyond 0·1 s. The improvements are spread across the frequency range 0–25 Hz, except near to the invariant points in suspension deflection and body acceleration, at which control cannot influence frequency responses [24]. The tyre deflection response dip for the active suspension at 13 Hz corresponds to the actuator, by virtue of the preview control, applying just sufficient force to the wheel to keep its centre a more or less constant distance from the ground. Clearly, the semi-active systems are inherently incapable of behaving in this way and there are no corresponding response valleys for these cases.

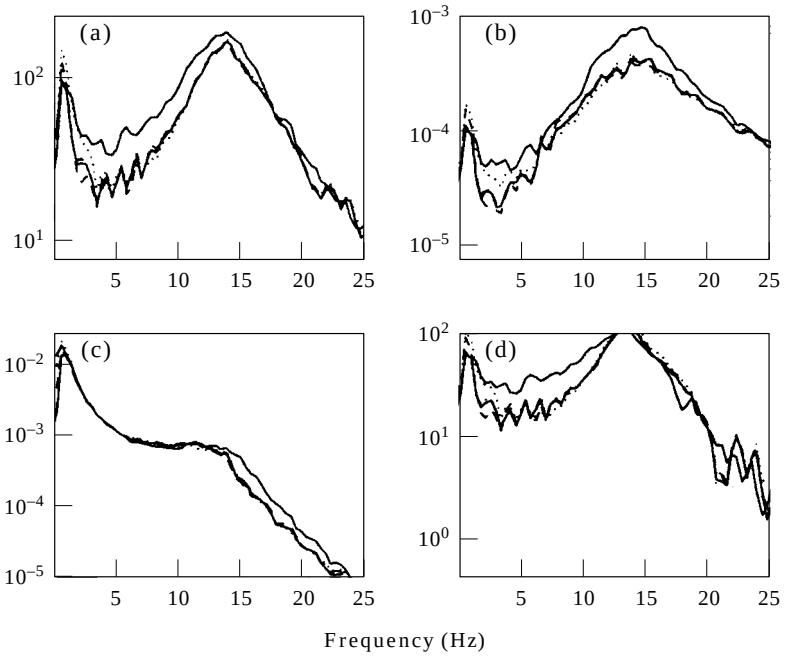

Figure 8. Output spectral densities for *CSN* system under white noise road velocity excitation for preview times (s) 0 (——), 0·1 (· · · ·), 0·25 (—), 0·5 (·–·–), 1·0 (——). (a) Total cost (1/Hz); (b) tyre deflection (m^2/Hz); (c) suspension deflection (m^2/Hz); (d) body acceleration ($(m\ s^{-2})^2$/Hz).

To illustrate further the operation of the semi-active systems, the proportions of the total time which they spend at their upper and lower coefficient constraint limits are shown in Figure 12.

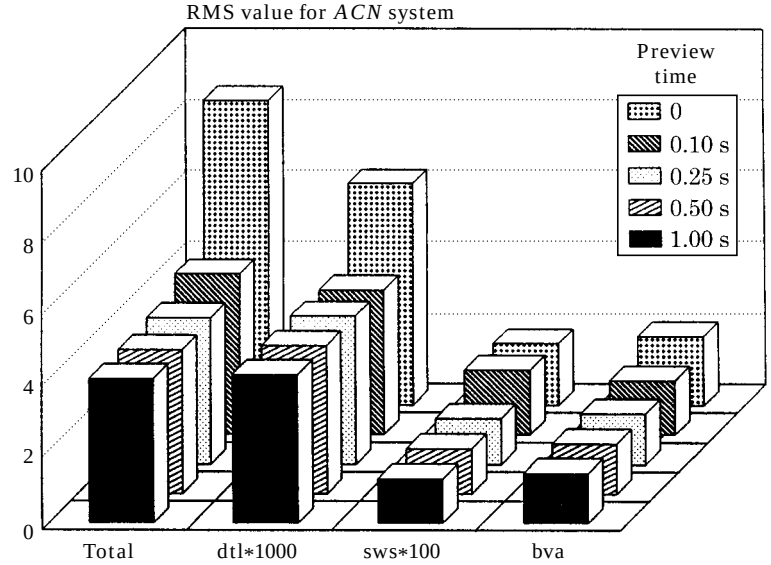

Figure 9. Bar chart showing RMS responses to white noise road velocity excitation for *ACN* systems.

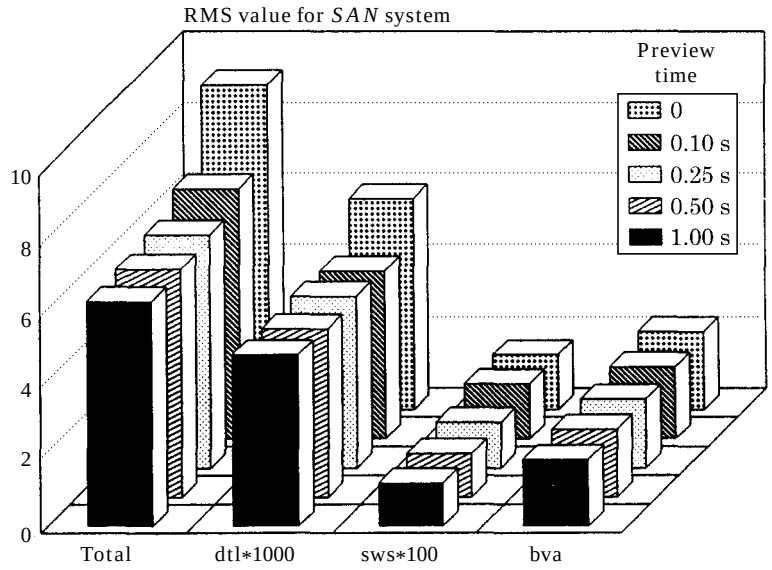

Figure 10. Bar chart showing RMS responses to white noise road velocity excitation for *SAN* systems.

Since the upper constraint limits are hardly used, it is clear that the systems are not significantly limited by the restriction placed on the dampers in respect of their ability to generate high forces for small velocities. The "soft" limits are used more often but still not a very high proportion of the total time. Whenever the globally optimal force generator would be doing work on the system, the best the semi-active system can do is to set the damping on the lower constraint limit, so

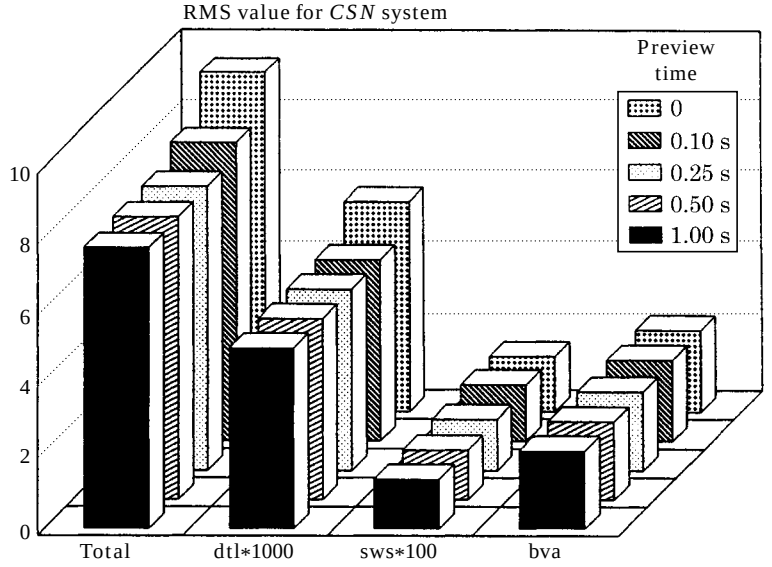

Figure 11. Bar chart showing RMS responses to white noise road velocity excitation for *CSN* systems.

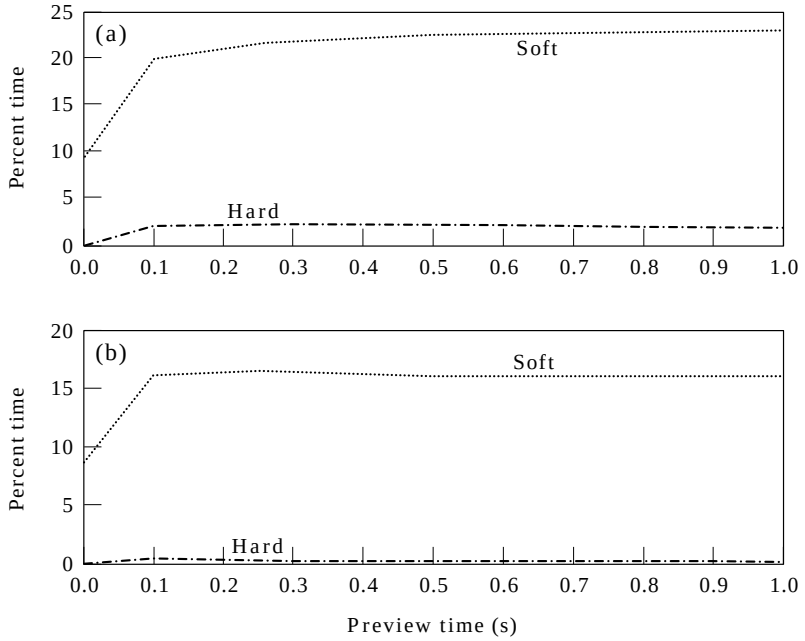

Figure 12. Proportions of total task time spent by (a) the optimally controlled damper and (b) the clipped controlled damper at high and low setting limits, as functions of the preview time.

it is reassuring to find this happening quite rarely. The distinct tendency is for it to happen more as the preview increases, which is entirely consistent with previous findings relating energy consumption in an active suspension to preview time [3, 5]. These increases in time spent at the "soft" limit, as the preview is extended, align with the increasing performance differences between active and semi-active systems.

4. CONCLUSIONS

A new frequency response function based analytical scheme for the establishment of the optimal capability of a linear system has been derived and it has been applied to finding the limits of an idealized quarter-car suspension with unlimited preview of the random disturbance provided by the road ahead.

A novel numerical optimization procedure, which is generally applicable to continuous non-linear systems, has been applied to various suspension optimization tasks; linear system results match those from alternative analyses, confirming the efficacy of the method. The procedure has yielded the optimal performance of semi-active suspensions with elastic damper mounting, damper force limits, high bandwidth operation and specified road preview times. Based on this realistic representation of a contemporary controllable damper and its installation in a road vehicle, and concentrating on the vibration isolation function of the suspension, it has been deduced that significant benefits are available from preview of the road. The benefits are however less than those obtainable from a corresponding full bandwidth active suspension. The major benefits are derived

from the first 0·1 s preview with the fast system considered but obtaining such preview information, for normal vehicle speeds, is non-trivial. The benefit is mainly in wheel load control. As the preview increases, the optimal system spends an increasing proportion of its total time on the "soft" limit. A feature of the numerical optimization procedure is that it is computationally very heavy for direct application to a running vehicle, at least in its current formulation.

Clipped optimal control is easier to implement in practice than the numerical scheme described and the loss of performance associated with it is small for the zero preview case. This is very much in tune with the findings of reference [13]. As the preview distance increases, clipped optimal control continues to improve performance as compared with the zero preview case but it loses ground systematically in relation to the numerically optimized systems, doing particularly badly at low frequencies. Neither semi-active system suffers a significant performance loss from the upper constraint placed on the damping coefficient, since very small proportions of the total time are spent at that limit, under the running conditions considered.

These results indicate that the "proof" of optimality of clipped optimal control for semi-active systems with preview in reference [11] does not apply to those cases considered here.

REFERENCES

1. E. K. Bender 1968 *Trans. ASME Journal of Basic Engineering* **90**(2), 213–221. Optimal linear preview control with application to vehicle suspension.
2. M. Tomizuka 1976 *Trans. ASME Journal of Dynamic Systems, Measurement and Control* **98**(3), 309–315. Optimal linear preview control with application to vehicle suspension—revisited.
3. R. S. Sharp 1995 in *Smart Vehicles* (J. P. Pauwelussen and H. B. Pacejka, editors); Lisse: Swets & Zeitlinger, 166–182. Preview control of active suspensions.
4. T. Morita, T. Tanaka, N. Kishimoto and M. Kishi 1992 *Proceedings of AVEC* '92, *SAE of Japan*, 111–116. Ride comfort improvement using preview sensors.
5. R. S. Sharp and C. Pilbeam 1996 *Vehicle System Dynamics* **25**(3), 169–183. Performance potential and power consumption of slow-active suspension systems with preview.
6. A. Hac 1992 *Vehicle System Dynamics* **21**(3), 167–195. Optimal linear preview control of active vehicle suspension.
7. Y. Araki, M. Oya and H. Harada 1994 *Proceedings of AVEC* '94, *SAE of Japan*, 299–304. Preview control of active suspension using disturbance of front wheel.
8. P. Hillebrecht, D. Konik, D. Pfeil, H. Wallentowitz and F. Zieglmeier 1992 *FISITA Congress Proceedings*, *Vol*. 2, *Total Vehicle Dynamics*; London: Mech. Eng. Publ., 221–230. The active suspension between customer benefit and technological competition.
9. M. B. Goran, B. I. Bachrach and R. E. Smith 1992 *FISITA Congress Proceedings*, *Vol*. 2, *Total Vehicle Dynamics*; London: Mech. Eng. Publ., 231–252. The design and development of a broad bandwidth active suspension concept car.
10. R. A. Williams and S. A. Miller 1994 *Proceedings of ICSE Conference*, *Coventry*. Power consumption in automotive active suspensions.
11. A. Hac and I. Youn 1992 *Proceedings ASME Journal of Vibration and Acoustics* **114**, 84–92. Optimal semi-active suspension with preview based on a quarter car model.

12. L. Jezequel and V. Roberti 1992 *Proceedings AVEC* '92, *SAE of Japan*, 123–129. Study of a nonlinear preview semi-active suspension system.
13. H. E. Tseng and J. K. Hedrick 1994 *Vehicle System Dynamics* **23**(7), 545–569. Semi-active control laws—optimal and sub-optimal.
14. J. H. E. A. Muijderman, F. E. Veldpaus and J. J. Kok 1994 *Proceedings AVEC* '94, *SAE of Japan*, 177–182. A semi-active suspension system based on dynamic programming.
15. J. H. E. A. Muijderman, F. E. Veldpaus, J. J. Kok and J. G. A. M. van Heck 1996 *Proceedings AVEC*'96, *Institute of Automotive Engineering*, *RWTH Aachen*, 63–75. A general criterion controller with preview for a semi-active truck suspension.
16. D. A. Wilson, R. S. Sharp and S. A. Hassan 1986 *Vehicle System Dynamics* **15**(2), 105–118. The application of linear optimal control theory to the design of active automotive suspensions.
17. T. J. Gordon, L. Palkovics, C. Pilbeam and R. S. Sharp 1994 in *Dynamics of Vehicles on Roads and Tracks* (Z. Y. Shen, editor). Lisse: Swets & Zeitlinger, *Vehicle System Dynamics*, *Vol*. 23 *Supplement*, 158–171. Second generation approaches to active and semi-active suspension control system design.
18. A. E. Bryson and Yu-Chi Ho 1975 *Applied Optimal Control*: *Optimization*, *Estimation and Control*. Washington: Hemisphere.
19. K. Ogata 1995 *Discrete—Time Control*. Englewood Cliffs, NJ: Prentice-Hall International, second edition.
20. T. J. Gordon and M. C. Best 1994 *CONTROL* '94 *IEE Conference Publication* 389, 332–337. Dynamic optimization of nonlinear semi-active suspension controllers.
21. T. J. Gordon 1995 *Chaos*, *Solitons and Fractals* **5**(9), 1603–1617. Non-linear optimal control of a vehicle suspension system.
22. G. Prokop and R. S. Sharp 1995 *IEE Proceedings*, *Control Theory and Applications* **142**(2), 140–148. Performance enhancement of limited bandwidth active automotive suspensions by road preview.
23. R. S. Sharp and S. A. Hassan 1986 *Proceedings of the Institution of Mechanical Engineers*, *Part D*, *Journal of Automobile Engineering* **200**, 219–228. The relative performance capabilities of active, passive and semi-active car suspension systems.
24. J. K. Hedrick and T. Butsuen 1988 *Advanced Suspensions*, *Proceedings of the Institution of Mechanical Engineers Conference*, *Mech*. *Eng*. *Publ*., 35–42. Invariant properties of automotive suspensions.

APPENDIX: DYNAMIC EQUATIONS AND COST FUNCTIONS

(A) ACTIVE SYSTEM

The active system is formulated by using the state variables

$$x_1 = z_r - z_w, \qquad x_2 = z_w - z_b, \qquad x_3 = \dot{z}_w, \qquad x_4 = \dot{z}_b, \tag{A1}$$

from which the state equations are easily found. Using the form

$$\dot{x} = f(x, u, w) \tag{A2}$$

of equation (16), one finds the right-hand side function:

$$f_1 = \dot{z}_r(t) - x_3, \qquad f_2 = x_3 - x_4, \qquad f_3 = (k_t x_1 - u)/M_w, \qquad f_4 = u/M_b. \tag{A3}$$

From equation (2) the cost function (19) is given by

$$L = \alpha x_1^2 + \beta x_2^2 + M_b^{-2} u^2. \tag{A4}$$

The co-state dynamic equations (21) take the form

$$\dot{p}_1 = -k_t p_3/M_w - 2\alpha x_1, \qquad \dot{p}_2 = -2\beta x_2,$$
$$\dot{p}_3 = p_1 - p_2, \qquad \dot{p}_4 = p_2. \tag{A5}$$

The linear passive system, used only for final co-state evaluation, is obtained from equations (A3) by setting $\dot{z}_r = 0$ and substituting the passive control force $u = k_s x_2 + b_s(x_3 - x_4)$, with damping rate $b_s = 1000$ N/(m s^{-1}) assumed; reference to equation (23) gives

$$A = \begin{vmatrix} 0 & 0 & -1 & 0 \\ 0 & 0 & 1 & -1 \\ 6{\cdot}67 * 10^3 & -667 & -33{\cdot}3 & 33{\cdot}3 \\ 0 & 80 & 4 & -4 \end{vmatrix}. \tag{A6}$$

Matrix Q in equation (24) becomes

$$Q = \begin{vmatrix} 116\,000 & 0 & 0 & 0 \\ 0 & 7590 & 320 & -320 \\ 0 & 320 & 16 & -16 \\ 0 & -320 & -16 & 16 \end{vmatrix}. \tag{A7}$$

From these the solution to equation (27) is found to be

$$P = \begin{vmatrix} 4{\cdot}58 * 10^3 & 957 & -8{\cdot}70 & 8{\cdot}70 \\ 957 & 1{\cdot}14 * 10^3 & -0{\cdot}974 & -55{\cdot}6 \\ -8{\cdot}70 & -0{\cdot}974 & 0{\cdot}495 & -0{\cdot}192 \\ 8{\cdot}70 & -55{\cdot}6 & -0{\cdot}192 & 17{\cdot}5 \end{vmatrix}. \tag{A8}$$

(B) SEMI-ACTIVE SYSTEM

In the semi-active system, the suspension force is written as

$$F = F_{\text{spring}} + F_{\text{damper}} = k_s(z_w - z_b) + \mu(v, \tilde{u}), \tag{A9}$$

where $\mu(v, \tilde{u})$ is the non-linear damper map, v is the relative velocity across the damper, and $\tilde{u}$ is the (filtered) control signal to the actuator. Upon writing x_d for the dynamic deflection of the compliant bush, the force balance between the bush and the damper implies

$$\mu(v, \tilde{u}) = k_c x_d.$$

Differentiation with respect to time implies:

$$\frac{\partial \mu}{\partial v}\dot{v} + \frac{\partial \mu}{\partial \tilde{u}}\dot{\tilde{u}} = k_c \dot{x}_d. \tag{A10}$$

The state equations for the semi-active system can now be formulated, upon using the same state variables as for the active system, taken together with

$$x_5 = v, \qquad x_6 = \tilde{u}, \qquad x_7 = \dot{\tilde{u}}. \tag{A11}$$

In the following the first of the partial derivatives in equation (A10) is abbreviated to μ_v and the second to μ_u. Then

$$f_1 = \dot{z}_r(t) - x_3, \qquad f_2 = x_3 - x_4, \qquad f_3 = (k_t x_1 - \mu - k_s x_2)/M_w,$$
$$f_4 = (\mu + k_s x_2)/M_b, \qquad f_5 = (k_c(x_3 - x_4 - x_5) - \mu_u x_7)/\mu_v,$$
$$f_6 = x_7, \qquad f_7 = \omega_n^2(u - x_6) - 2\zeta\omega_n x_7. \tag{A12}$$

Note that the first four equations are essentially the same as for the active system, but with equation (A6) used in place of u. The fifth equation follows from equation (A10), upon first noting that $\dot{x}_d$ can be written as $(x_3 - x_4 - x_5)$. The last two equations are just the filter dynamics for the controllable damper. The cost function becomes

$$L = \alpha x_1^2 + \beta x_2^2 + M_b^{-2}(\mu + k_s x_2)^2 + \gamma u^2, \tag{A13}$$

where the additional term γu^2 is included for reasons of numerical stability; with $\gamma = 10^{-5}$, and u restricted to the range $(0, 100)$; its magnitude is negligible compared to the other terms. As a matter of detail, $\tilde{u}$ is allowed to overshoot the limits (0, 100), though this occurs only rarely, and for very short periods of time.

Now the co-state dynamic equations (21) take the form

$$\dot{p}_1 = -k_t p_3/M_w - 2\alpha x_1,$$
$$\dot{p}_2 = k_s p_3/M_w - k_s p_4/M_b - 2\beta x_2 - 2k_s M_b^{-2}(\mu + k_s x_2),$$
$$\dot{p}_3 = p_1 - p_2 - k_c p_5/\mu_v, \qquad \dot{p}_4 = p_2 + k_c p_5/\mu_v,$$
$$\dot{p}_5 = \mu_v p_3/M_w - \mu_v p_4/M_b - 2\mu_v(\mu + k_s x_2)M_b^{-2} \cdots$$
$$+ \mu_{vv}\mu_v^{-2} p_5(k_c(x_3 - x_4 - x_5) - \mu_u x_7) + p_s(k_c + \mu_{vu} x_7)/\mu_v$$
$$\dot{p}_6 = \mu_u p_3/M_w - \mu_u p_4/M_b + \omega_n^2 p_7 - 2\mu_u(\mu + k_s x_2)M_b^{-2} \cdots$$
$$+ \mu_{uu} p_5 x_7/\mu_v + \mu_{vu}\mu_v^{-2} p_5(k_c(x_3 - x_4 - x_5) - \mu_u x_7),$$
$$\dot{p}_7 = \mu_u p_5/\mu_v - p_6 + 2\zeta\omega_n p_7. \tag{A14}$$

Final co-states are found via an expanded P matrix,

$$P_7 = \left[\begin{array}{c|c} P & 0_{4,3} \\ \hline 0_{3,4} & 0_{3,3} \end{array}\right] \tag{A15}$$

where $0_{4,3}$ is a 4×3 matrix of zeros, and P is given above in equation (A8).